Article
Vol. 25, No. 4, p. 417–431, August 2021
https://doi.org/10.1007/s12303-020-0044-5
pISSN 1226-4806 eISSN 1598-7477
Geosciences Journal GJ

The Ordovician succession of the Taebaek Group (Korea) revisited: old conodont data, new perspectives, and implications

Se Hyun Cho[1], Byung-Su Lee[2], Dong-Jin Lee[3], and Suk-Joo Choh[1]*

[1]Department of Earth and Environmental Sciences, Korea University, Seoul 02841, Republic of Korea
[2]Department of Earth Science Education, Chonbuk National University, Jeonju 54896, Republic of Korea
[3]College of Earth Sciences, Jilin University, Changchun 130061, China

ABSTRACT: We recompiled available Ordovician conodont data from previous studies for the Taebaek Group of the Taebaeksan Basin, Korea, based on the recently revised Ordovician conodont biostratigraphic scheme for North China. The recompiled Ordovician Taebaek Group conodont data conform well with the middle Tremadocian, lower Floian, and middle Darriwilian biozones of North China. The overall conodont distribution patterns, the occurrence of endemic species found only in North China, and the presence of an Upper Ordovician hiatus reaffirms the close relationship of the Taebaeksan Basin to the North China (Sino-Korean) Block. In addition, the absence of middle Floian to lower Darriwilian conodonts in the Taebaek Group and sudden appearance of abundant middle Darriwilian conodonts raises the possibility of the presence of a hiatus in the Lower Ordovician of the Taebaek Group. The possible disconformity may be located at the uppermost contact of the massive dolostone interval (the basal member) of the Makgol Formation. Lithologic evidence for the discontinuity includes the presence of local brecciation and oversized vuggy pores immediately below the contact and that of numerous dolomitic clasts above the contact.

Key words: Ordovician, conodont biostratigraphy, Taebaek Group, North China, Makgol Formation

Manuscript received June 25, 2020; Manuscript accepted September 7, 2020

1. INTRODUCTION

The Ordovician was a period of rapid diversification of organisms, dynamic long-term warm to cool global climate change, and plate reorganization around the paleo-Tethys and Iapetus oceans (Cooper et al., 2012). The tripartite subdivision of the Ordovician System into the Lower, Middle, and Upper series was ratified by the International Commission of Stratigraphy (ICS) in the 1990s, and was followed by establishment of seven international stages based primarily on the first appearance of specific graptolite or conodont species (Cooper et al., 2012; Bergström and Ferretti, 2017). Conodonts are "tooth-like" elements composed of hydroxylapatite, formerly part of the feeding apparatus of conodont animals, preserved in shallow shelf carbonate deposits of Cambrian to Triassic age and have been mostly used for biostratigraphic correlation within a region. However, recent attempts of international correlation to utilize pandemic species have been made (Bergström and Ferretti, 2017).

The Ordovician conodont fauna of the North China (Sino-Korean) Block is known to be markedly composed of endemic species, compared to the assemblages of Siberia, South China, Australia, which surrounded North China during the early Paleozoic (Wang et al., 2016). However, utilization of the widely distributed species, such as *Histiodella holodentata* (Ethington and Clark, 1981), enabled a breakthrough that led to reevaluation and redefinition of the previous Ordovician conodont biostratigraphy of North China over the last five years (Wang et al., 2016; Wang et al., 2018). Notable progress based on this revision of biozones included reconfirmation and temporal extension of a platform-wide hiatus within the Lower to Middle Ordovician deposits (Wang et al., 2016; Zhen et al., 2016).

The possibility of these significant findings being applicable to the Taebaeksan Basin of the Korean Peninsula has not yet been addressed. The conodont fauna of the Joseon Supergroup

*Corresponding author:
Suk-Joo Choh
Department of Earth and Environmental Sciences, Korea University, Seoul 02841, Republic of Korea
Tel: +82-2-3290-3180, Fax: +82-2-3290-3189, E-mail: sjchoh@korea.ac.kr

in the Taebaeksan Basin has been suggested as closely related to that of the North China bioprovince (Lee and Lee, 1986; Lee and Lee, 1990); therefore, the recent major changes in the conodont biostratigraphic scheme of North China also need to be tested in the Taebaeksan Basin. In this study, we recompiled and rearranged all available Ordovician conodont data from the Taebaek Group documented in previous studies, according to the revised Ordovician conodont biozones of North China, and discuss its potential geologic implications.

2. GEOLOGIC SETTING AND METHODS

The geological succession of the Taebaeksan Basin of the central-eastern Korean Peninsula consists of the mixed clastic-carbonate Joseon Supergroup, which rests nonconformably on metamorphic rocks of the Precambrian Yeongnam Massif and is disconformably overlain by clastic rocks of the upper Paleozoic Pyeongan Supergroup (Fig. 1). The Joseon Supergroup is divided into the Taebaek, Yeongwol, Yongtan, Pyeongchang, and Mungyeong groups on the basis of their geographic distributions, among which paleontological studies have mostly been conducted on the Taebaek and Yeongwol groups (Choi, 1998). The Taebaek Group is composed of eleven lithostratigraphic units: the Jangsan/Myeonsan, Myobong, Daegi, Sesong, Hwajeol, Dongjeom, Dumugol, Makgol, Jigunsan, and Duwibong formations in ascending stratigraphic order (Chough, 2013).

The first conodont study of the Joseon Supergroup was conducted in 1964 by Müller; subsequently, the late Prof. H.-Y. Lee and his colleagues began to investigate the Joseon Supergroup conodonts in earnest from the 1970s (Lee and Seo, 2004). Conodont studies of the Taebaek Group indicated that the Sesong and Hwajeol formations are upper Cambrian (Lee, 2014; Lee and Bak, 2015), whereas the Dumugol-Duwibong formations are Ordovician (Lee and Seo, 2004).

The current study focuses on conodont data obtained from Ordovician strata of the Taebaek Group that crop out around the Taebaek and Yeongwol areas (Hwang, 1986; Lee, 1986; Lee and Lee, 1986; Kim, 1987; Lee and Lee, 1990; Seo et al., 1994; Lee, 2009; Seo and Lee, 2010). These Ordovician strata of the Taebaek Group are composed of limestone and shale alternations of the Dumugol Formation, massive dolostone and peritidal to subtidal limestone of the Makgol Formation, fine-grained clastic dominated Jigunsan Formation, and subtidal limestone deposits of the Duwibong Formation (Choi et al., 2004; Chough, 2013). We recompiled conodont distribution data for the Lower to Middle Ordovician Taebaek Group, with particular reference to the key species used for establishment of the recently revised biozones of North China (Wang et al., 2014; Wang et al., 2016; Wang et al., 2018), and compared the result with the platform-wide conodont biostratigraphy. Because the thickness of each

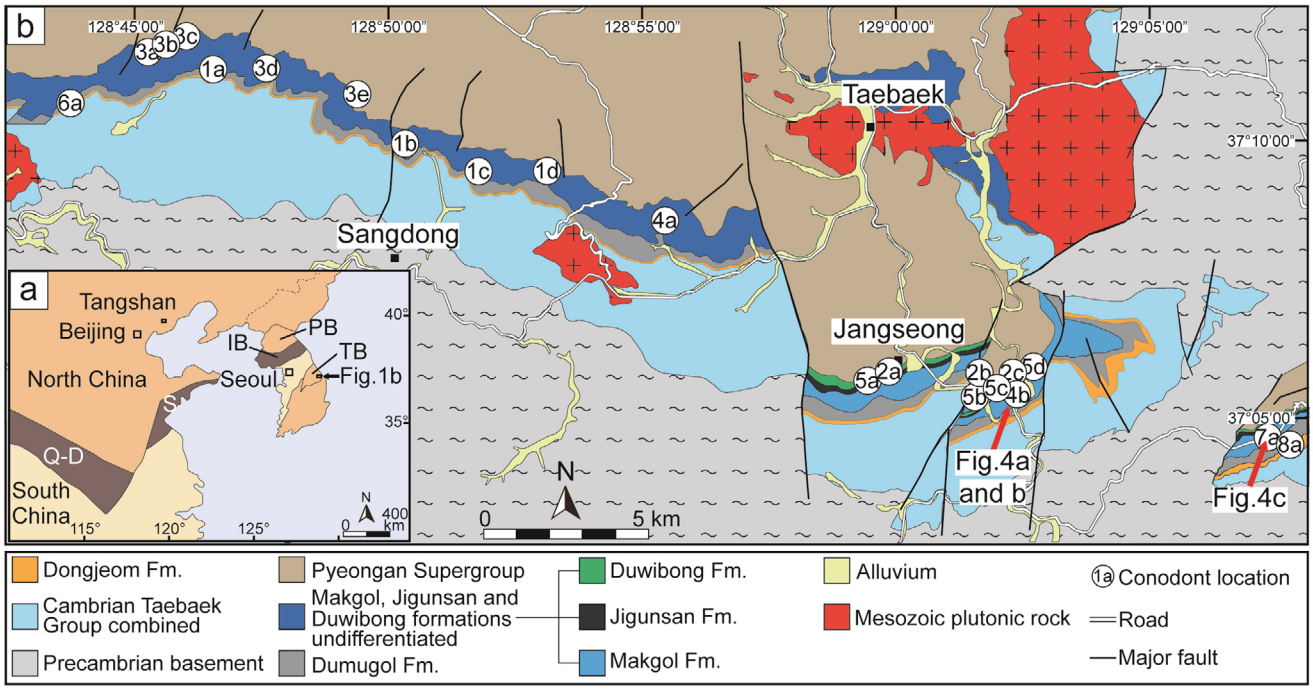

Fig. 1. (a) Tectonic map of the North China (Sino-Korean) and South China blocks. IB, Imjingang Belt; S, Sulu Belt; Q-D, Qingling-Dabie Belt; PB, Pyeongnam Basin; TB, Taebaeksan Basin (Chough, 2013; Zheng et al., 2013). (b) Geologic map of the study area and conodont-occurring localities. Alphanumeric symbols refer to the locations of sections in each reference used in this study: 1, Hwang, 1986; 2, Lee, 1986; 3, Lee and Lee, 1986; 4, Kim, 1987; 5, Lee and Lee, 1990; 6, Seo et al., 1994; 7, Lee, 2009; 8, Seo and Lee, 2010.

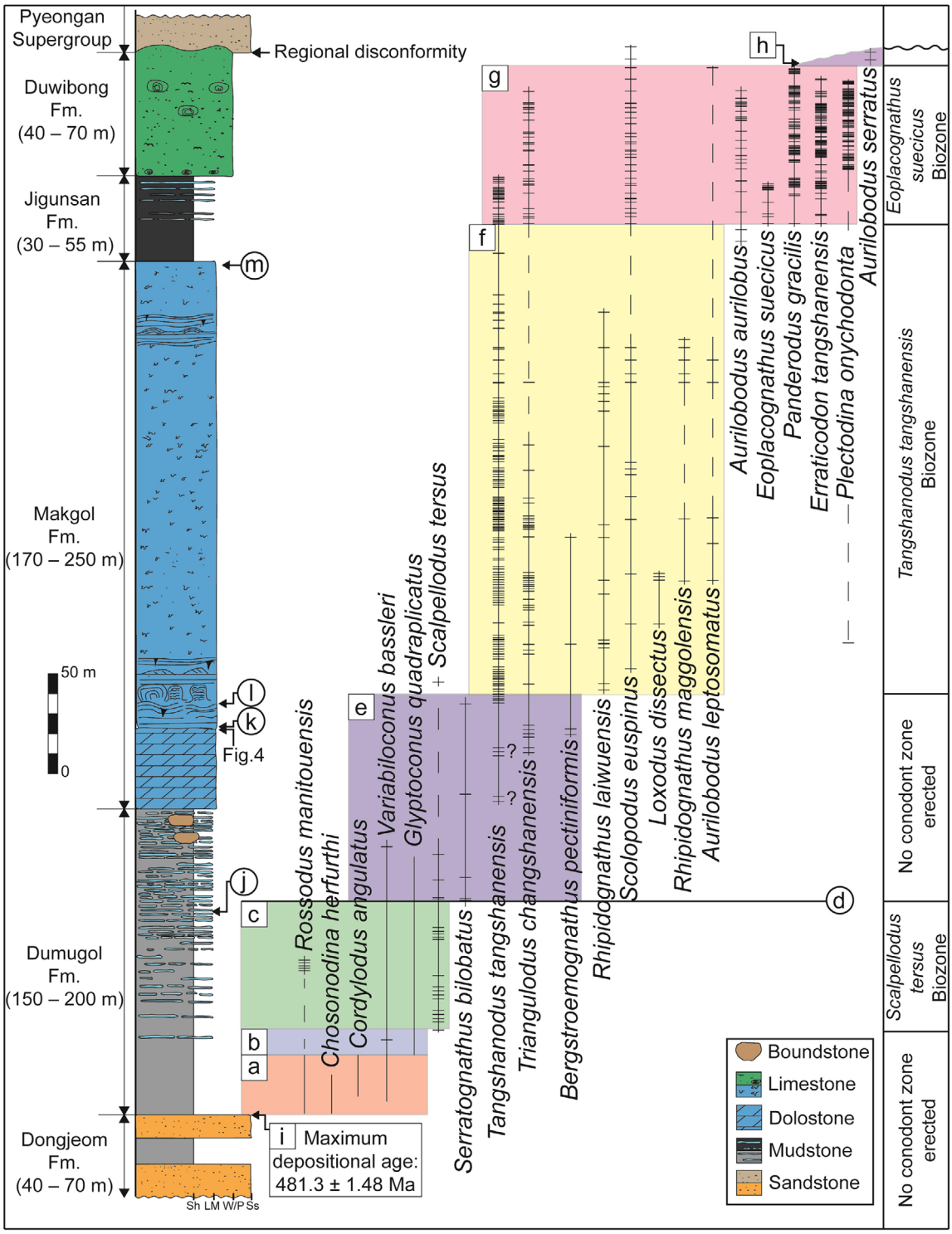

Fig. 2. Composite section of the Ordovician Taebaek Group with the vertical distributions of principal conodont species from previously published studies and unpublished data. Dashes in vertical line indicate the conodont-yielding horizons and vertical dashed lines depict that the conodont-yielding horizons are more than 50 m apart. (a–h) Conodont groups classified by index species and assemblage. (a) Typical conodonts indicating a middle Tremadocian age. (b) Poorly defined interval at the lower Dumugol Formation. (c) *Scalpellodus tersus* Biozone, defined from the first appearance datum (FAD) of *Scalpellodus tersus* to the FAD of *S. bilobatus*. (d) Tremadocian–Floian boundary, defined by the FAD of *S. bilobatus*. (e) Poorly defined interval from the upper Dumugol Formation to the lower Makgol Formation. (f) *Tangshanodus tangshanensis* Biozone, defined by *Tangshanodus tangshanensis* and the associated assemblage. (g) *Eoplacognathus suecicus* Biozone, defined from the FAD of *Eoplacognathus suecicus* to the FAD of *Aurilobodus serratus* and the last appearance datum (LAD) of *Plectodina onychodonta*. (h) Above the *Eoplacognathus suecicus* Biozone, uppermost Duwibong Formation in the Gumunso section. (i–m) Occurrence of graptolites, trilobites, and cephalopods, and zircon age data. (i) Zircon dating of the uppermost Dongjeom Formation (Kim et al., 2019). (j) Graptolites in the upper Dumugol Formation (Kwon, 2007). (k, l, m) Cephalopods in the Makgol Formation (Yun, 1999).

https://doi.org/10.1007/s12303-020-0044-5

formation changes laterally across the study area, we constructed the composite section utilizing the boundary between each formation as datum for correlation between the locations (Fig. 2). The boundary between Dumugol and Makgol formations was used as datum for compilation of the conodont occurrence data of the five studies (Hwang, 1986; Kim, 1987; Seo et al., 1994; Lee, 2009; Seo and Lee, 2010), and similarly, the boundaries between Makgol and Jigunsan formations and, Jigunsan and Duwibong formations, were used as the datum for compilation of those of the three studies (Lee, 1986; Lee and Lee, 1986; Lee and Lee, 1990).

It should be noted that descriptions of the lithologic boundary between the Dumugol and Makgol formations are not consistent among previous studies. Some studies designated an approximately 60-m-thick interval consisting of bioturbated wackestone-packstone, limestone-shale couplets, limestone pebble conglomerate, and bioherms with sponges as the lower member of the Makgol Formation, and the immediately overlying massive dolostone interval as the middle member (Paik, 1987; Woo, 1999). In contrast, others incorporated this "lower member" of the Makgol Formation into the upper member of the Dumugol Formation, regarding the base of the massive dolostone interval (the "middle member" of the Makgol Formation) as the boundary between the two formations (Kwon et al., 2003; Choi et al., 2004), primarily based on ease of recognition in field mapping. Choi et al. (2004) subdivided the Makgol Formation into the basal, lower, middle, and upper members, with the massive dolostone interval corresponding to the basal member. This scheme was followed in the present study.

3. NEW CONSTRAINTS ON CONODONT DATA

3.1. Brief History of Chinese Conodont Studies (1970s to the Present)

Studies of Chinese Ordovician conodonts started in the late 1970s (Wang et al., 2018), and preliminary results provided the basis for the definition of biozones in several regions of China. The first Ordovician conodont biozonation of North China, comprising 13 biozones, was erected by An et al. (1983); this scheme was further revised by Wang and Wang (1983) and Wang et al. (1996). It has been noted that the conodont biozonation of China shows regional differences: although Tremadocian (early Early Ordovician) conodonts show similar species assemblages across the region, younger conodonts exhibit distinct differences in northern and southern China, which prompted delineation of the North and South China conodont bioprovinces (Wang et al., 1996). Although the South China conodont biozones are similar to those of Baltoscandia, those of North China contain many endemic species, as well as some pandemic species common to the North American Midcontinent conodont fauna (Wang et al., 1996). As conodonts inhabiting shallow, warm-water environments tend to be more endemic than those from cool, deeper-water environments, the North China bioprovince was interpreted to have been deposited in shallow, warm-water environments (Bergström and Ferretti, 2017); thus, the North China conodont biozones are less useful for regional and international correlation (Wang et al., 2018). To resolve this shortcoming, several attempts have been made since the 1990s, including integration of conodont and graptolite biozones in mixed siliciclastic and carbonate facies, allowing for more robust correlation with the Upper Ordovician successions of North America and Baltoscandia (Wang et al., 2013). In addition, *Pygodus* and *Periodon*, cosmopolitan conodonts from the slope setting of western North China, have been successfully used as replacements for the endemic index species of previous late Middle to Upper Ordovician biozones, such as the *Aurilobodus serratus*, *Scandodus handanensis*, and *Tasmanognathus sishuiensis* biozones (Jing et al., 2015).

Histiodella holodentata, formerly reported as *Histiodella infrequensa* in the Bei'anzhuang Formation (formerly the lower Majiagou Formation) of Tangshan, Hebei Province, North China (An et al., 1983), was recently re-examined (Wang et al., 2014). The Bei'anzhuang Formation was previously interpreted as Dapingian (early Middle Ordovician) to early Darriwilian in age (An et al., 1983). *Histiodella holodentata* was first reported from the middle Darriwilian of the Table Head Group, Newfoundland, Canada (Stouge, 1984), then from the Middle Ordovician of Oklahoma, USA (Bauer, 2010). This taxon is one of the key species of the Middle Ordovician North American Midcontinent conodont biozonation (Bergström and Ferretti, 2017), and is widely distributed across North America, Baltoscandia, the Argentine Precordillera, and South China (Stouge, 1984; Bergström and Ferretti, 2017). The prominent biostratigraphic significance of this species prompted a major revision of Ordovician conodont biostratigraphy of North China. The previous Dapingian to early Darriwilian *Aurilobodus leptosomatus* and *Tangshanodus tangshanensis* biozones were merged into the *Histiodella holodentata–Tangshanodus tangshanensis* Biozone, and redesignated as a middle Darriwilian biozone. This led to the conclusion that the "Huaiyuan Epeirogeny" entrained another event to produce a disconformity between the Lower and Middle Ordovician in North China, in addition to widely recognized mid-Paleozoic great hiatus (Zhen et al., 2016).

3.2. Revised Ordovician Conodont Biozones of North China

The revised Ordovician conodont biostratigraphy of North China consists of 23 biozones, incorporating the Dapingian to

Table 1. Summary of revised North China Ordovician conodont biozones

		Revised North China conodont biozonal scheme (Wang et al., 2016)			
		Biozone	Lower boundary	Upper boundary	Assemblage
Ordovician	445 Ma				
	Katian	*Y. yaoxianensis* Biozone	FAD of *Y. yaoxianensis*	Unclear	*Y. yaoxianensis*, Be. confluens, Ou. tunguskaensis*, Ph. undatus, Ps. dispansa, Tao. blandus, Y. lijiapoensis*, Y. neimengguensis**
		Y. neimengguensis Biozone	FAD of *Y. neimengguensis*	FAD of *Y. yaoxianensis*	*Y. neimengguensis*, Be.compressa, Be. confluens, Ph. undatus, Pr. insculptus, Ps. dispansa, Tao. blandus, Y. lijiapoensis*, D. mutatus, Ou. tunguskaensis**
	453 Ma	*Be. confluens* Biozone	FAD of *Be. confluens*	FAD of *Y. neimengguensis*	*Be. confluens, Be. compressa, Ou. tunguskaensis*, Ph. undatus, Ps. dispansa, Tao. blandus*
	Sandbian	*Ph. undatus* Biozone	FAD of *Ph. undatus*	FAD of *Be. confluens*	*Ph. undatus, Be. compressa, Ou. tunguskaensis*, Scab. altipes*
		Be. compressa Biozone	FAD of *Be. compressa*	FAD of *Ph. undatus*	*Be. compressa, Tas. sishuiensis*, Eri. typus, Mi. symmetricus*
		Eri. quadridactylus Biozone	FAD of *Eri. quadridactylus*	FAD of *Be. compressa*	*Eri. quadridactylus, Co. ethingtoni, Eo. sp., Pan. gracilis, Pe. aculeatus, Pe. grandis, Pr. rectus, Pr. robustus, Pr. varicostatus, Spi. spinatus*
		Pl. aculeata Biozone	FAD of *Pl. aculeata*	FAD of *Eri. quadridactylus*	*Pl. aculeata, Co. ethingtoni, Eo. sp., Pan. Gracilis, Pe. Aculeatus*
	458 Ma	*Py. anserinus* Biozone	FAD of *Py. anserinus*	FAD of *Pl. aculeata*	*Py. anserinus, D. viruensis, Pe. aculeatus, Pr. varicostatus*
	Darriwilian	*Py. serra* Biozone	FAD of *Py. serra*	FAD of *Py. anserinus*	*Py. serra, D. viruensis, Pe. aculeatus, Pr. varicostatus*
		Py. anitae Biozone	FAD of *Py. anitae*	FAD of *Py. serra*	*Py. anitae, An. jemtlandica, Cor. longibasis, Co. ethingtoni, D. viruensis, Eo. suecicus, Pan. gracilis, Pe. fabellum, Pr. cooperi, Pr. varicostatus, Spi. spinatus*
		Eo. suecicus Biozone	FAD of *Eo. suecicus* or *H. kristinae*	LAD of *Pl. onychodonta*	*Eo. suecicus, H. kristinae, Eo. pseudoplanus, Er. tangshanensis*, T. changshanensis*, A. linxiensis**
		H. holodentata-Tan. tangshanensis Biozone	FAD of *H. holodentata* or *Tan. tangshanensis*	FAD of *Eo. suecicus* or *H. kristinae*	*H. holodentata, Tan. tangshanensis*, Au. leptosomatus, L. dissectus*, R. maggolensis, R. laiwuensis*, T. changshanensis**
	467 Ma				
	Dap.		Hiatus		
	470 Ma				
	Floian	*J. gananda* Biozone	FAD of *J. gananda*	Unclear	*J. gananda, B. hubeiensis, B. extensus, Sco. euspinus**
		Pa. obesus Biozone	FAD of *Pa. obesus* or *Pa. paltodiformis*	FAD of *J. gananda*	*Pa. obesus*, Pa. paltodiformis, B. pectiniformis*, Pa. problematicus*, R. maggolensis*
		S. extensus Biozone	FAD of *S. extensus*	FAD of *Pa. obesus* or *Pa. paltodiformis*	*S. extensus, B. extensus, B. hubeiensis, O. multidentatus*, S. bilobatus*
	477 Ma	*S. bilobatus* Biozone	FAD of *S. bilobatus*	FAD of *S. extensus*	*S. bilobatus, B. extensus, O. multidentatus*, T. aff. bifidus**
	Tremadocian	*Sca. tersus-T.* aff. *bifidus* Biozone	FAD of *Sca. tersus*	FAD of *S. bilobatus*	*Sca. tersus*, T. aff. bifidus*, G. quadraplicatus*
		G. quadraplicatus Biozone	FAD of *G. quadraplicatus*	FAD of *Sca. tersus* or *T.* aff. *bifidus*	*G. quadraplicatus, Alo. staufferi, Ro. manitouensis*
		Ro. manitouensis Biozone	FAD of *Ro. manitouensis*	FAD of *G. quadraplicatus*	*Ro. manitouenesis, Alo. staufferi, Ch. herfurthi, C. angulatus, V. bassleri*
		Ch. herfurthi Biozone	FAD of *Ch. herfurthi*	FAD of *Ro. manitouensis*	*Alo. staufferi, C. angulatus, V. bassleri*
		C. angulatus Biozone	FAD of *C. angulatus*	FAD of *Ch. herfurthi*	*C. angulatus, C. drucei, C. intermedius, C. lindstromi, M. sevierensis*
	485 Ma	*I. jilinensis-C. lindstromi* Biozone	FAD of *I. jilinensis* or *C. lindstromi*	FAD of *C. angulatus*	*Alb. postcostatus*, C. caseyi, C. drucei, C. intermedius, C. proavus, M. sevierensis, U. utahensis*

Asterisks (*) indicate species endemic to North China; Dap. = Dapingian.

Abbreviation of generic name: *A.* = *Acontiodus?*; *Alb.* = *Albiconus*; *Alo.* = *Aloxoconus*; *An.* = *Ansella*; *Au.* = *Aurilobodus*; *B.* = *Bergstroemognathus*; *Be.* = *Belodina*; *C.* = *Cordylodus*; *Ch.* = *Chosonodina*; *Co.* = *Costiconus*; *Cor.* = *Cornuodus*; *D.* = *Dapsilodus*; *Eo.* = *Eoplacognathus*; *Er.* = *Erraticodon*; *Eri.* = *Erismodus*; *G.* = *Glyptoconus*; *H.* = *Histiodella*; *I.* = *Iapetognathus*; *J.* = *Jumudontus*; *L.* = *Loxodus*; *M.* = *Monocostodus*; *Mi.* = *Microcoelodus*; *O.* = *Oistodus*; *Ou.* = *Oulodus*; *Pa.* = *Paraserratognathus*; *Pan.* = *Panderodus*; *Pe.* = *Periodon*; *Ph.* = *Phragmodus*; *Pl.* = *Plectodina*; *Pr.* = *Protopanderodus*; *Ps.* = *Pseudobelodina*; *Py.* = *Pygodus*; *R.* = *Rhipidognathus*; *Ro.* = *Rossodus*; *S.* = *Serratognathus*; *Sca.* = *Scalpellodus*; *Scab.* = *Scabbardella*; *Sco.* = *Scolopodus*; *Spi.* = *Spinodus*; *T.* = *Triangulodus*; *Tan.* = *Tangshanodus*; *Tao.* = *Taoqupognathus*; *Tas.* = *Tasmanognathus*; *U.* = *Utahconus*; *V.* = *Variabiloconus*; *Y.* = *Yaoxianognathus*.

https://doi.org/10.1007/s12303-020-0044-5

lower Darriwilian and upper Katian to Mississippian hiatuses (Wang et al., 2016; Wang et al., 2018). The lower limits of each biozone are based mainly on the first appearance datum (FAD) or the last appearance datum (LAD) of the index species, and subordinately by the stratigraphic ranges of coexisting species (Table 1). The following is a brief description of the current conodont biozones in each stage of the North China succession, as recently revised by Wang et al. (2018).

The global Cambrian–Ordovician boundary (the base of the Tremadocian) is defined by the FAD of the conodont *Iapetognathus fluctivagus* at the Green Point section in western Newfoundland, Canada (Cooper et al., 2001). *Iapetognathus fluctivagus* has not been reported from North China; in that area, the base of the Ordovician System was established on the basis of the FAD of *Cordylodus lindstromi* and *Iapetognathus jilinensis*, species closely related to *I. fluctivagus* (Wang et al., 2016; Wang et al., 2018). Tremadocian biozones across North China were established using the widely distributed species *I. jilinensis*, *C. lindstromi*, *Cordylodus angulatus*, *Chosonodina herfurthi*, *Rossodus manitouensis*, and *Glyptoconus quadraplicatus*, as well as the endemic species *Scalpellodus tersus* and *Triangulodus* aff. *bifidus* as index species (Table 1; Wang et al., 2016; Wang et al., 2018).

The global base of the Floian Stage is defined as the FAD of the graptolite *Tetragraptus approximatus*, occurring within conodont *Paroistodus proteus* Biozone at the Diabasbrottet section in southwest Sweden (Bergström et al., 2004). In South China, *Paroistodus proteus* has been only reported in slope facies, in which it coexists with *Serratognathus diversus*. As *Paroistodus proteus* has not been reported in platform carbonates, the base of the Floian is marked by the FAD of *S. diversus* in those environments (Wang et al., 2019). In North China, neither *Paroistodus proteus* nor *S. diversus* have been discovered, thus the FAD of *Serratognathus bilobatus*, a species closely related to *S. diversus*, is used to define the base of the Floian Stage (Zhen et al., 2015; Wang et al., 2018). Subsequently, the Floian and lower Dapingian successions of North China are subdivided into the *S. bilobatus*, *Serratognathus extensus*, *Paraserratognathus obesus*, and *Jumudontus gananda* biozones in ascending order (Wang et al., 2016; Wang et al., 2018).

Middle Dapingian to lower Darriwilian strata are absent across North China (Zhen et al., 2016), and the *Histiodella holodentata–Tangshanodus tangshanensis* Biozone (middle Darriwilian) is defined above the disconformity (Table 1; Wang et al., 2014). The lower and upper boundaries of this biozone are marked by the FAD of *H. holodentata* or *Tangshanodus tangshanensis*, and that of *Eoplacognathus suecicus* or *Histiodella kristinae*, respectively (Wang et al., 2016). However, the lower boundary of this biozone does not necessarily correspond to the first occurrence of *H. holodentata* or *Tangshanodus tangshanensis*, due to the sedimentary discontinuity between the Darriwilian and the underlying strata (Wang et al., 2016). The conodont assemblage of the biozone also contains *Aurilobodus leptosomatus*, *Loxodus dissectus*, *Rhipidognathus maggolensis*, *Rhipidognathus laiwuensis*, and *Triangulodus changshanensis* (Wang et al., 2016; Wang et al., 2018). Other Darriwilian biozones above the *Histiodella holodentata–Tangshanodus tangshanensis* Biozone were established using the cosmopolitan species *Eoplacognathus suecicus*, *Pygodus anitae*, and *Pygodus serra*. *Pygodus anitae* and *Pygodus serra* occur in the slope facies of western North China (Table 1; Jing et al., 2015; Wang et al., 2016; Wang et al., 2018).

The global base of the Sandbian Stage is defined as the FAD of the graptolite *Nemagraptus gracilis* at the Fågelsång section in southern Sweden (Bergström et al., 2000). A comparative study of conodont and graptolite distributions in Sweden indicated that the FAD of *N. gracilis* is located in the middle part of the *Pygodus anserinus* Biozone (Bergström, 2007). *Pygodus anserinus* has been reported from the slope deposits of western North China, and the *Pygodus anserinus* Biozone was regarded as being correlatable with the *Tasmanognathus sishuiensis* Biozone, defined in the platform carbonates of southern and northern North China (Jing et al., 2015). The Sandbian biozones above the *Pygodus anserinus* Biozone include the *Plectodina aculeata*, *Erismodus quadridactylus*, *Belodina compressa*, and *Phragmodus undatus* biozones, in ascending order. This sequence of biozones is somewhat similar to those of the North American Midcontinent and South China (Bergström and Ferretti, 2017). Most Sandbian biozones of North China, except the *Belodina compressa* Biozone that is recognized in Fengfeng of Henan Province and Pingliang of Gansu Province were established in western North China, as Sandbian strata are absent from southern and northern North China (Wang et al., 2018).

The global base of the Katian Stage is defined as the FAD of the graptolite *Diplacanthograptus caudatus* at the Black Knob Ridge section in southeastern Oklahoma (Goldman et al., 2007). In studies of conodont biozonation, the lower boundary of the *Plectodina tenuis* Biozone in the North American Midcontinent was suggested as the base of the Katian (Saltzman et al., 2014; Zhen and Percival, 2017). Although *Plectodina tenuis* has not been reported in North China, *Belodina confluens*, the index species of the *Belodina confluens* Biozone above the *Plectodina tenuis* Biozone in the North American Midcontinent, has been found in western North China; therefore, the base of the Katian Stage is considered to occur beneath the first occurrence horizon of *Belodina confluens* (Wang et al., 2016; Wang et al., 2018). The Katian conodont biozones of North China include, in ascending order, the *Belodina confluens*, *Yaoxianognathus neimengguensis*, and *Yaoxianognathus yaoxianensis* biozones. These biozones are recognized only in western North China; middle to upper

Katian strata are absent across North China (Wang et al., 2016; Wang et al., 2018).

4. APPLICATION OF THE NORTH CHINA BIOSTRATIGRAPHIC SCHEME TO THE TAEBAEK GROUP

4.1. Conodonts of the Ordovician Taebaek Group

In the Taebaek Group, the late Furongian *Monocostodus sevierensis* was reported from the uppermost Hwajeol Formation (Lee, 1992; Lee and Bak, 2015); however, *I. fluctivagus* and *C. lindstromi*, indicator species of the base of the Tremadocian, have not yet been reported. Instead, *Rossodus manitouensis*, *Chosonodina herfurthi*, *C. angulatus*, and *Variabiloconus bassleri*, indicating a middle Tremadocian age, have been found at the base of the Dumugol Formation overlying the sandstone-dominated Dongjeom Formation (interval "a" in Fig. 2; Seo et al., 1994). Even though *G. quadraplicatus*, the index species of the late Tremadocian biozone in North China, first occurs in the lower Dumugol Formation, a biozone was not formally erected because no conodonts other than *V. bassleri* have been found (interval "b" in Fig. 2; Seo et al., 1994). Approximately 10 m above the first occurrence horizon of *G. quadraplicatus*, *Scalpellodus tersus* occurs with *G. quadraplicatus* and *V. bassleri* (Hwang, 1986; Kim, 1987), which allows the establishment of the *Scalpellodus tersus* Biozone (interval "c" in Fig. 2). *Serratognathus bilobatus*, an indicator species for the base of the Floian Stage in North China, first appears in the upper Dumugol Formation (horizon "d" in Fig. 2; Hwang, 1986). As other species typically associated with *S. bilobatus* in other continents have not been found, formal establishment of a biozone is not possible at present. Similarly, *S. extensus*, *Paraserratognathus obesus*, and *J. gananda*, the index species of the Floian and Dapingian in North China, have not been reported from the Taebaek Group.

Conodont recovery is very poor from the massive dolostone interval (the basal member) of the Makgol Formation, although unpublished data indicate rare (fewer than 5 elements/kg of sample) occurrences of *S. bilobatus* and *Tangshanodus tangshanensis* (interval "e" in Fig. 2; Kim, 1987; Lee, 2009); thus, biozone establishment is not feasible for this interval at present. In contrast, *Tangshanodus tangshanensis*, *Aurilobodus leptosomatus*, *L. dissectus*, *R. maggolensis*, *R. laiwuensis*, and *T. changshanensis* have been abundantly recovered from cyclic limestone strata in the lower to upper member of the Makgol Formation (interval "f" in Fig. 2; Kim, 1987; Lee, 2009). As these taxa are common constituents of the *Histiodella holodentata–Tangshanodus tangshanensis* Biozone of North China (Wang et al., 2014), and *Tangshanodus tangshanensis* is the index species of this biozone, the *Tangshanodus tangshanensis* Biozone was established from the lower member of the Makgol Formation to lower Jigunsan Formation (interval "f" in Fig. 2).

Eoplacognathus suecicus, which defines the upper boundary of the *Histiodella holodentata–Tangshanodus tangshanensis* Biozone of North China (Wang et al., 2018), first occurs in the middle Jigunsan Formation, and the co-occurrence of *Tangshanodus tangshanensis*, *T. changshanensis*, *Scolopodus euspinus*, *Aurilobodus leptosomatus*, *Aurilobodus aurilobus*, *Panderodus gracilis*, and *Erraticodon tangshanensis* (Lee and Lee, 1986; Lee and Lee, 1990) allows the establishment of the *Eoplacognathus suecicus* Biozone (interval "g" in Fig. 2). The conodont fauna of the Duwibong Formation is similar to that of the Jigunsan Formation, except for the disappearance of *Tangshanodus tangshanensis* and *Eoplacognathus suecicus,* and the appearance of *Aurilobodus serratus* (interval "g and h" in Fig. 2; Lee and Lee, 1986; Lee and Lee, 1990).

It should be noted that the uppermost parts of the Taebaek Group show differing conodont distributions from area to area in the Taebaeksan Basin. *Aurilobodus serratus* is the index species of the *Aurilobodus serratus* Biozone that overlies the *Eoplacognathus suecicus* Biozone in northern and southern North China; the *Aurilobodus serratus* Biozone is correlated with the *Pygodus anitae* Biozone of western North China (Jing et al., 2015). In Napalgogae section (Dongjeom-dong) and Jikdong area (2d, 3a, and 5d in Fig. 1b), based on the occurrence of *Aurilobodus serratus* in the uppermost part of the Duwibong Formation, the *Aurilobodus serratus* Biozone was established (interval "h" in Fig. 2; Lee, 1986; Lee and Lee, 1986; Lee and Lee, 1990). In contrast, *Aurilobodus serratus* has not been reported from, and *Plectodina onychodonta* is usually found in, the uppermost Duwibong Formation in all other areas in the Taebaeksan Basin, indicating that the upper limit of the formation is still within the *Eoplacognathus suecicus* Biozone (Lee, 1986; Lee and Lee, 1986; Lee and Lee, 1990). Such differences in the spatial distributions of conodonts indicate that the upper boundary of the Taebaek Group is largely controlled by an uneven erosive surface (Lee et al., 2017).

The revised Ordovician conodont biostratigraphy of the Taebaek Group is summarized in Figures 2, 3 and Table 2. In the Dumugol Formation, the sequential appearance of *Rossodus manitouensis*, *G. quadraplicatus*, *Scalpellodus tersus*, and *S. bilobatus* is well correlated with the middle Tremadocian and early Floian biozones of North China. The paucity of conodonts in the basal member of the Makgol Formation prevents formal establishment of a conodont biozone. However, *Tangshanodus tangshanensis*, *Eoplacognathus suecicus*, and associated species in the overlying lower member of the Makgol Formation to Duwibong Formation are remarkably similar to the middle–late Darriwilian conodont biozones of northern North China (Wang et al., 2016). Thus, the middle Floian to early Darriwilian fauna is highly likely to be absent from the Taebaek Group, similarly to North China, where a hiatus from the middle Dapingian to lower Darriwilian

https://doi.org/10.1007/s12303-020-0044-5

Table 2. Conodont occurrence data in the Taebaek Group (See Table 1 for abbreviations)

Group	Formation	Section (location in Fig. 1b)	Geographic coordinate	Occuring index taxa	Occurring assemblage	Source
Taebaek	Duwibong	Palgu (3e)	37°10'33"N, 128°48'44"E	*Pl. onychodonta*	*Er. tangshanensis* *Pan. gracilis* *Au. aurilobus* *Sco. euspinus*	Lee and Lee (1986)
	Duwibong, Jigunsan	Dumudong valley (3a, 3b and 3c)	37°11'34"N, 128°44'39"E, 37°11'34"N, 128°45'29"E	*Au. serratus* *Pl. onychodonta* *Eo. suecicus* *Tan. tangshanensis*		
	Jigunsan	Wooseong Mine (3d)	37°11'22"N, 128°46'48"E	*Tan. tangshanensis*	*Er. tangshanensis* *Pan. gracilis*	
	Duwibong, Jigunsan, Makgol	Geumcheon (2a and 5a)	37°06'00"N, 129°00'07"E	*Pl. onychodonta* *Eo. suecicus* *Tan. tangshanensis*	*Er. tangshanensis* *Pan. gracilis* *Au. aurilobus* *Sco. euspinus* *T. changshanensis*	Lee (1986); Lee and Lee (1990)
		Napalgogae (2d and 5d)	37°05'58"N, 129°02'49"E	*Au. serratus* *Pl. onychodonta* *Eo. suecicus* *Tan. tangshanensis*	*Er. tangshanensis* *Pan. gracilis* *Au. aurilobus* *Au. leptosomatus* *R. maggolensis* *Sco. euspinus* *R. laiwuensis* *T. changshanensis*	
	Duwibong, Jigunsan	Memiltle (2b and 5b)	37°05'43"N, 129°01'26"E	*Pl. onychodonta* *Eo. suecicus* *Tan. tangshanensis*	*Er. tangshanensis* *Pan. gracilis* *Au. aurilobus* *Sco. euspinus* *T. changshanensis*	
	Jigunsan, Makgol	Hyeolnaechon (2c and 5c)	37°05'46"N, 129°02'15"E	*Eo. suecicus* *Tan. tangshanensis*	*Er. tangshanensis* *Sco. euspinus* *R. laiwuensis*	
	Jigunsan, Makgol, Dumugol	Guraeri (1d)	37°09'15"N, 128°52'28"E	*Eo. suecicus* *Tan. tangshanensis* *S. bilobatus* *Sca. tersus*	*Au. leptosomatus* *L. dissectus* *T. changshanensis*	Hwang (1986)
	Makgol, Dumugol	Jikdongri(1a)	37°11'03"N, 128°45'33"E	*Tan. tangshanensis* *S. bilobatus* *Sca. tersus*	*Au. leptosomatus* *R. maggolensis* *Sco. euspinus* *R. laiwuensis* *T. changshanensis*	
		Teoggol (1b)	37°09'53"N, 128°49'33"E	*S. bilobatus* *Sca. tersus*		
		Danyangchon (1c)	37°09'19"N, 128°51'10"E	*Tan. tangshanensis* *S. bilobatus* *Sca. tersus*	*T. changshanensis*	
	Makgol, Dumugol	Seokgaejae (7a and 8a)	37°04'56"N, 129°07'59"E	*Pl. onychodonta* *Tan. tangshanensis* *Sca. tersus*	*R. laiwuensis* *B. pectiniformis* *T. changshanensis* *V. bassleri*	Lee (2009); Seo and Lee (2010)
	Makgol, Dumugol	Sanaegol (4a)	37°08'19"N, 128°55'26"E	*Tan. tangshanensis* *Sca. tersus*	*Au. leptosomatus* *R. maggolensis* *L. dissectus* *Sco. euspinus* *R. laiwuensis* *B. pectiniformis* *T. changshanensis*	Kim (1987)
		Dongjeom (4b)	37°05'35"N, 129°02'31"E	*Tan. tangshanensis*	*R. maggolensis* *L. dissectus* *Sco. euspinus* *R. laiwuensis* *B. pectiniformis* *T. changshanensis*	
	Dumugol	Maggol (6a)	37°10'36"N, 128°42'31"E	*G. quadraplicatus* *C. angulatus* *Ch. herfurthi* *Ro. manitouensis*	*V. bassleri*	Seo et al. (1994)

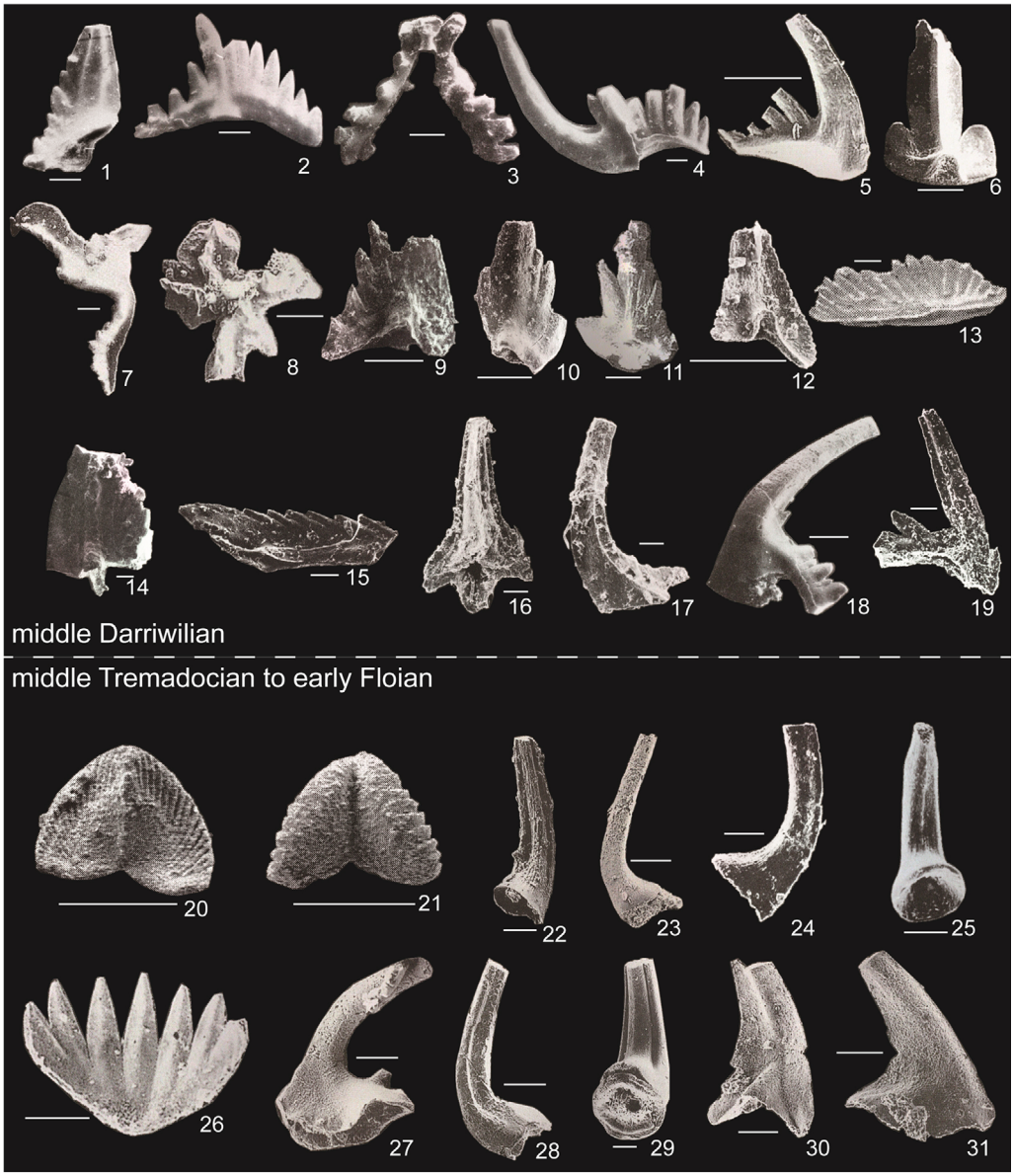

Fig. 3. Representative conodont species of the Dumugol to Duwibong formations of the Taebaek Group. (1) *Aurilobodus serratus* Xian & Zhang, 1983, asymmetricus element, posterior view, Duwibong Formation (Lee and Lee, 1986) (2 and 3) *Plectodina onychodonta* An & Xu, 1983; 2, prioniodiniform element, lateral view, Duwibong Formation (Lee and Lee, 1986); 3, trichonodelliform element, posterior view, Duwibong Formation (Lee and Lee, 1986). (4 and 5) *Erraticodon tangshanensis* Yang & Xu, 1983; 4, hindeodelliform element, lateral view, Duwibong Formation (Lee and Lee, 1986); 5, cordylodontiform element, postero-lateral view, Duwibong Formation (Lee and Lee, 1990). (6) *Aurilobodus aurilobus* Lee, 1975, symmetricus element, posterior view, Duwibong Formation (Lee and Lee, 1990). (7 and 8) *Eoplacognathus suecicus* Bergström, 1971; 7, dextral ambalodontiform element, Jigunsan Formation (Lee and Lee, 1986); 8, polyplacognathiform element, Jigunsan Formation (Lee and Lee, 1990). (9–11) *Rhipidognathus maggolensis* Lee, 1976; 9, bryantodiniform element, posterior view, Makgol Formation (Kim, 1987); 10, trichonodelliform element, posterior view, Makgol Formation (Kim, 1987); 11, bryantodiniform element, lateral view, Makgol Formation (Lee and Lee, 1990). (12) *Aurilobodus leptosomatus* An, 1983, posterior view, Makgol Formation (Kim, 1987). (13) *Rhipidognathus laiwuensis* Zhang, 1983, bryantodiniform element, posterior view, Makgol Formation (Lee, 2009). (14 and 15) *Bergstroemognathus pectiniformis* Yang & Zhang, 1983; 14, trichonodelliform element, posterior view, Makgol Formation (Kim, 1987); 15, falodontiform element, lateral view, Makgol Formation (Kim, 1987). (16 and 17) *Triangulodus changshanensis* Zhang, 1983; 16, oistodontiform element, posterior view, Makgol Formation (Kim, 1987); 17, trichonodelliform element, lateral view, Makgol Formation (Kim, 1987). (18 and 19) *Tangshanodus tangshanensis* An, 1983. 18, Cordylodontiform element, Jigunsan Formation (Lee and Lee, 1986); 19, prioniodiniform element, lateral view, Makgol Formation (Kim, 1987). (20 and 21) *Serratognathus bilobatus* Lee, 1970; 20, lateral view, Makgol Formation (Lee, 2009); 21, lateral view, Makgol Formation (Lee, 2009). (22 and 23) *Glyptoconus quadraplicatus* Branson & Mehl, 1933; 22, postero-lateral view, Dumugol Formation (Seo et al., 1994); 23, lateral view, Dumugol Formation (Seo et al., 1994). (24 and 25) *Scalpellodus tersus* Zhang F., 1983; 24, scandodontiform element, lateral view, Makgol Formation (Kim, 1987); 25, acontiodontiform element, posterior view, Makgol Formation (Kim, 1987). (26) *Chosonodina herfurthi* Müller, 1964, concave side view, Dumugol Formation (Seo et al., 1994). (27) *Cordylodus angulatus* Pander, 1856, lateral view, Dumugol Formation (Seo et al., 1994). (28 and 29) *Variabiloconus bassleri* Furnish, 1938; 28, lateral view, Dumugol Formation (Seo et al., 1994); 29, postero-lateral view, Dumugol Formation (Seo et al., 1994). (30 and 31) *Rossodus manitouensis* Repetski and Ethington, 1983; 30, acontiodiform element, postero-lateral view, Dumugol Formation (Seo et al., 1994); 31, drepanodiform element, lateral view, Dumugol Formation (Seo et al., 1994). All scale bars are 0.1 mm.

https://doi.org/10.1007/s12303-020-0044-5

is recognized (Fig. 3).

4.2. Other Fossils of the Ordovician Taebaek Group

The recompiled conodont data can be supplemented more precisely by integration of the available trilobite, graptolite, and cephalopod biostratigraphic data, and zircon age data from the Ordovician Taebaek Group. Recently obtained zircon ages from the uppermost Dongjeom Formation indicate a maximum depositional age of 481.3 ± 1.48 Ma, suggesting that the base of the Dumugol Formation corresponds to the middle to upper Tremadocian (horizon "i" in Fig. 2; Kim et al., 2019).

Even though the FAD of *S. bilobatus* was reported at the upper Dumugol Formation (Hwang, 1986), subsequent studies did not reproduced *S. bilobatus* and interpreted the upper Dumugol Formation as late Tremadocian (Table 2; Seo et al., 1994; Seo and Lee, 2010). Trilobites from the lower, upper, and uppermost Dumugol Formation are middle Tremadocian, late Tremadocian, and early Floian taxa, respectively (Kim et al., 1991). In addition, the graptolite *Hunnegraptus novus*, indicating the latest Tremadocian, occurs about 50 m below the boundary between the Dumugol and Makgol formations (horizon "j" in Fig. 2; Kwon, 2007). Because the results of all paleontologic studies are not consistent, it is suggested that integration of trilobite, graptolite, and conodont data is necessary for the accurate recognition of Tremadocian–Floian boundary in the Taebaek Group.

A cephalopod study has reported *Manchuroceras* sp., a common Floian cephalopod, from the uppermost basal member of the Makgol Formation (horizon "k" in Fig. 2; Yun, 1999). In addition, *Wutinoceras* sp. was found in the lowermost lower member of the Makgol Formation, which was correlated with the Bei'anzhuang Formation of North China that was formerly thought to be Dapingian in age (horizon "l" in Fig. 2; Yun, 1999). It should be noted that the Bei'anzhuang Formation is now regarded as Darriwilian in age as the result of revision of the North China Ordovician conodont biozonation (Wang et al., 2016; Wang et al., 2018). Cephalopods reported from the uppermost Makgol Formation (horizon "m" in Fig. 2; Yun, 1999), and graptolites and trilobites from the Jigunsan Formation (interval "f" in Fig. 2; Lee and Choi, 1992; Kim et al., 2005), are indicative of a Darriwilian age for the strata, which is in good agreement with the recompiled conodont data (Fig. 2 and Table 1).

5. IMPLICATIONS

5.1. Relationship between North China and the Taebaeksan Basin

Ordovician conodont biostratigraphy of South China has also been recently revised based on widely distributed taxa as index species (Wang et al., 2019). A total of 29 and 17 biozones have been established in the Yangtze Platform and Jiangnan Slope, respectively, and their correlation resulted in 28 Ordovician conodont biozones for South China (Zhen et al., 2014; Wang et al., 2019). The Middle to Late Ordovician conodont fauna of South China is very similar to the Baltoscandian fauna, but differs from those of North China and Australia in that it contains abundant deeper-water taxa (Wang et al., 2019).

In the case of the Taebaek Group, although *Chosonodina herfurthi*, *Variabiloconus bassleri*, and *Glyptoconus quadraplicatus*, which are found in the lower Dumugol Formation, are widely distributed Tremadocian species that have been reported throughout North America, South China, and North China (Repetski and Ethington, 1983; Miller et al., 2003; Wang et al., 2018; Wang et al., 2019), the conodont faunas of the middle to upper Dumugol, Makgol, Jigunsan, and Duwibong formations are particularly similar to those of North China, but differ distinctly from those of North America and South China. In particular, *Tangshanodus tangshanensis* and *Erraticodon tangshanensis* are endemic species specific to North China that do not occur in South China, but have been abundantly recovered from the Taebaek Group.

In addition to the Taebaek Group, the revised North China Ordovician conodont biozones can also be applied to delineate the relationship between the Taebaeksan Basin and North China (Table 3). Early to late Tremadocian conodonts including *C. lindstromi*, *Rossodus manitouensis*, and *Chosonodina herfurthi*, which occur in the lower part of the Dumugol Formation, have been reported from the Mungok Formation of the Yeongwol Group (Lee and Lee, 1999), and Darriwilian conodonts including *Erraticodon tangshanensis*, *Aurilobodus leptosomatus*, and *Scolopodus euspinus*, which are common in the middle member of the Makgol Formation to the Duwibong Formation, have been documented from the Yeongheung Formation (Lee, 1990). In the Mungyeong Group, *Panderodus gracilis*, which first appears in the upper Darriwilian rocks of North China, was documented in the eastern Mungyeong area (Lee et al., 1993). In the Yongtan Group of the Jeongseon area, *Panderodus gracilis*, *Erismodus quadridactylus*, and *Plectodina aculeata* have recently been recovered from the Hoedongri Formation (Lee, 2019). These Hoedongri conodonts are index and affiliated species of the Sandbian *Plectodina aculeata* and *Erismodus quadridactylus* biozones in North China. The occurrences of these species in the Yeongwol, Mungyeong, and Yongtan groups support the notion that the Ordovician conodonts of the Taebaeksan Basin are part of the typical North China conodont fauna.

The co-occurrence of endemic species and correlation of biozones indicate that the Taebaeksan Basin was biogeographically

Table 3. Conodont occurrence data in the Yeongwol, Mungyeong, and Yongtan groups (See Table 1 for abbreviations)

Group	Formation	Section/point	Geographic coordinate	Occuring index taxa	Occurring assemblage	Source
Yeongwol	Yeongheung	Bukssangri	37°12'17"N, 128°25'20"E	*Pl. onychodonta*	*Au. leptosomatus* *Sco. euspinus*	Lee (1990)
		Mungokri	37°15'22"N, 128°25'59"E		*Er. tangshanensis* *Sco. euspinus* *T. changshanensis*	
		Machari	37°17'30"N, 128°28'55"E		*Er. tangshanensis* *Pan. gracilis* *Sco. euspinus* *T. changshanensis*	
	Mungok	Golmacha	37°15'21"N, 128°26'48"E	*C. angulatus* *Ch.herfurthi* *Ro. manitouensis* *C. lindstromi*		Lee and Lee (1999)
		Seonghwangchon	37°17'07"N, 128°26'07"E	*C. angulatus* *Ch. herfurthi* *Ro. manitouensis*		
		Mohari	37°12'48"N, 128°26'07"E	*Sca. tersus* *Ro. manitouensis*		
Mungyeong	Bugokri	Hogyeri	36°40'25"N, 128°10'25"E	*Pl. onychodonta*	*Pan. gracilis* *Sco. euspinus*	Lee et al. (1993)
		Byeoramri	36°39'24"N, 128°10'43"E		*Au. leptosomatus* *Sco. euspinus* *T. changshanensis*	
		Bugokri	36°41'42"N, 128°11'24"E		*Pan. gracilis* *Er. tangshanensis* *Sco. euspinus*	
Yongtan	Hoedongri	Yami	37°25'03"N, 128°38'23"E	*Eri. quadridactylus*		Lee (2019)
		Seongmaryeong	37°23'24"N, 128°32'46"E	*Pl. aculeata*	*Pan. gracilis*	

closely related to North China during the Ordovician. In addition, an Upper Ordovician hiatus of similar magnitude occurs in both the Joseon Supergroup (Lee et al., 2017) and North China, in stark contrast to the Ordovician succession of South China, which does not contain any major hiatuses. Thus, the current study reaffirms the previous notion of the Taebaeksan Basin as a genetic eastern extension of North China.

5.2. Disconformity within the Ordovician Succession of the Taebaek Group?

In North China, disconformity between the Lower and Middle Ordovician has been recognized through conodont biostratigraphy and lithostratigraphic data, which has been interpreted to be caused by the "Huaiyuan Epeirogeny" (Zhang and Zhen, 1991; Zhen et al., 2016). On the other hand, similar discontinuity surface has not been recognized in the Joseon Supergroup. The recompiled conodont distributions of the Taebaek Group strongly indicate the presence of a previously unrecognized discontinuity spanning the middle Floian through lower Darriwilian. This discontinuity is located within the interval between the first appearance of *S. bilobatus* in the upper Dumugol Formation and the lower limit of the *Tangshanodus tangshanensis* Biozone in the Makgol Formation (Fig. 2). This potential interval is entirely composed of carbonate rocks without major variations in lithology, with no significant change in bedding directions. A discontinuity surface that bears such characteristics is a disconformity, which is typically accompanied by an irregular contact, erosional surface, paleosols, and gravels derived from underlying strata. The missing geologic record associated with a disconformity may only be reconstructed through paleontological evidence (Boggs, 2014).

The 30- to 50-m-thick massive dolostone interval (the basal member) of the Makgol Formation is overlain by the cyclic peritidal limestone of the lower member of the formation, which contains numerous subaerial exposure surfaces (Paik, 1987; Woo, 1999). In the Gumunso (Figs. 4a and b) and Seokgaejae (Fig. 4c) sections, the boundary of the massive dolostone and overlying limestone is sharp and irregular. The dolostone immediately below this surface is composed of bioturbated dolomitic mudstone and intraclastic packstone to grainstone, with local patchy development of vuggy to channel pores, and laterally restricted breccias with dolomitic or micritic matrix. Immediately above the boundary lies a conglomerate consisting of numerous dolomitic clasts of various sizes (up to 50 cm long), which show the same texture as the underlying dolostone and lime mudstone matrix, and include significant amounts of quartz sand. The presence of vuggy to channel pores in the uppermost part of the dolostone

https://doi.org/10.1007/s12303-020-0044-5

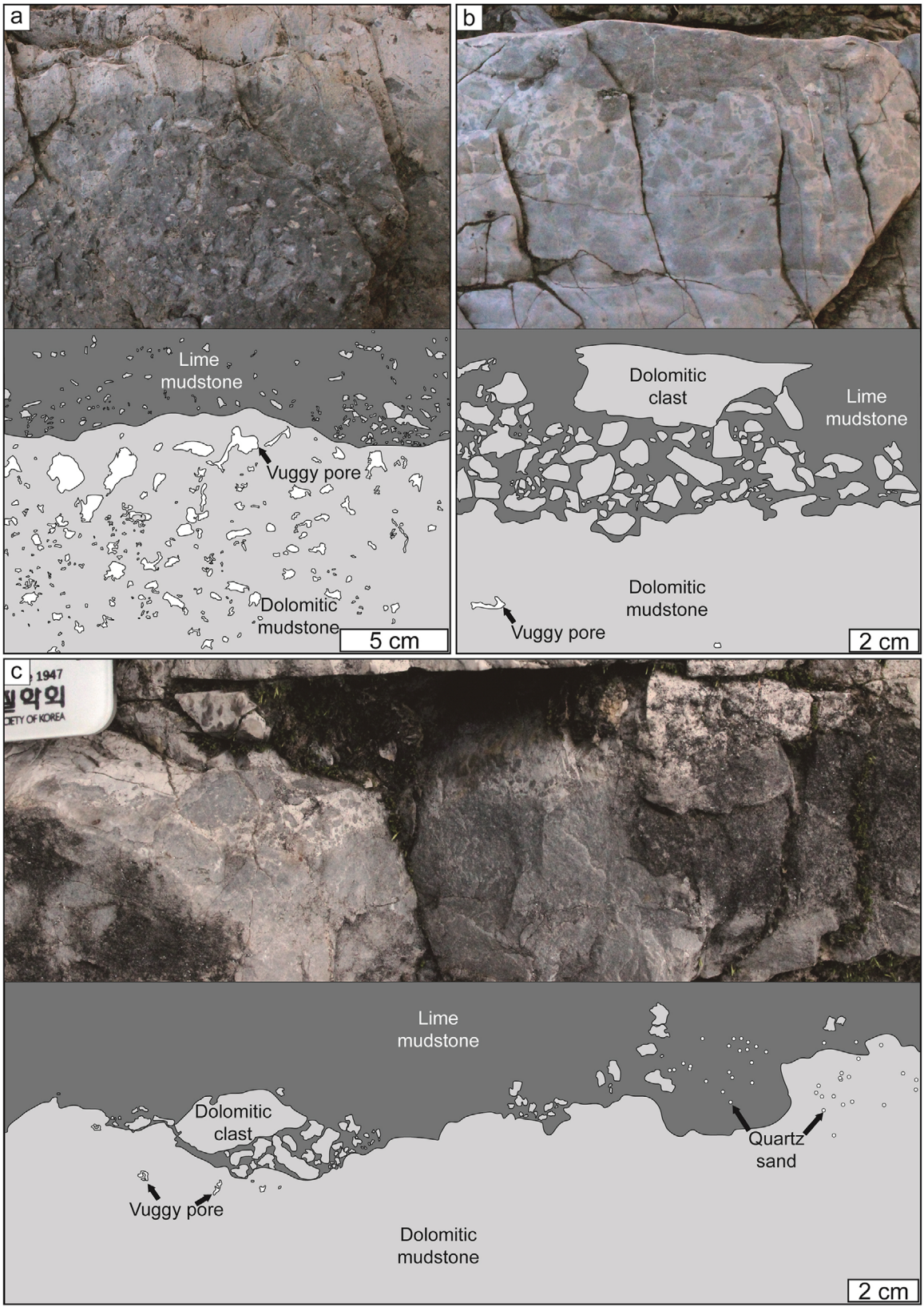

Fig. 4. Field photographs and sketches showing the uppermost boundary of massive dolostone (the basal member) in the Makgol Formation. (a) and (b) are from the Gumunso section, and (c) from the Seokgaejae section (see Fig. 1 for location of each section). Note the sharp, irregular boundary between dark gray dolomitic mudstone and overlying light gray lime mudstone; the upper part of the dark gray dolostone contains some oversized vuggy pores; the light gray limestone immediately overlying the irregular surface contains silt- to boulder-sized dolomitic clasts and silt to sand-sized quartz grains.

https://doi.org/10.1007/s12303-020-0044-5 https://www.springer.com/journal/12303

interval indicates selective to non-selective dissolution by meteoric water (Desrochers and James, 1988; Knight et al., 1991; Dix et al., 1998), whereas the numerous dolostone clasts indicate that the clasts originated from the underlying dolomitic interval after dolomitization (Mussman and Read, 1986; Cooper and Keller, 2001). These features are indicative of subaerial exposure, but intensity and duration required to produce the features were probably stronger and/or longer, compared to exposure features such as desiccation cracks and evaporite mineral casts (Cooper and Keller, 2001) that are observed in the overlying cyclic limestone deposited above the boundary (Paik, 1987; Woo, 1999). A detailed sedimentological description and the field relationships of the disconformity surface will be presented in a future study.

Although the available conodont biostratigraphic data and a small number of other studies make it possible to infer the presence of a hiatus within the Makgol Formation, further detailed paleontological investigations of the upper part of the Dumugol Formation and the basal member of the Makgol Formation are required to pinpoint the discontinuity surface; identification of this surface may be corroborated by sedimentological investigation. In addition, the similar overall absence of middle Floian to Dapingian conodonts in other groups of the Joseon Supergroup suggest that this hiatus may also exist across the Taebaeksan Basin; this possibility also warrants further study.

6. CONCLUSIONS

Recompiled Ordovician conodont data of the Taebaek Group, with reference to the recently revised conodont biostratigraphy of North China, demonstrate remarkable faunal similarities between the Taebaek Group and North China. The *Scalpellodus tersus* Biozone is established in the Dumugol Formation, and the overall conodont distributions are similar to those of middle to late Tremadocian and early Floian conodont biozones of North China. The paucity of conodont recovery prevents establishment of a conodont biozone in the basal member of the Makgol Formation. The *Tangshanodus tangshanensis* and *Eoplacognathus suecicus* biozones of the lower member of the Makgol Formation through the Duwibong Formation are well correlated with the middle to late Darriwilian conodont biozones of North China. *Tangshanodus tangshanensis*, *Erraticodon tangshanensis*, and *T. changshanensis*, which are endemic to North China, occur in abundance in the Taebaek Group. These occurrences reaffirm the close biogeographic link between the Taebaeksan Basin and North China. The recompiled conodont data also indicate for the first time an absence of middle to late Floian, Dapingian, and early Darriwilian conodonts in the Taebaek Group, implying a hiatus during this period. We suggest this previously unrecognized disconformity is located at the uppermost boundary of the massive dolostone interval (the basal member) of the Makgol Formation; numerous dolostone clasts are found above the sharp, irregular surface, whereas pockets of brecciated zones and vuggy pores are observed below the surface.

ACKNOWLEDGMENTS

This study was supported by grants from the National Research Foundation of Korea to SJC (2018R1A2A2A05018469), DJL (2018R1A2B2005578), and BSL (2020R1A2C1099624). The authors are grateful to reviewers Y.Y. Zhen (Geological Survey of New South Wales) and S.-B. Lee (Korea Institute of Geosciences and Mineral Resources) and handling editor D.C. Lee (Chungbuk National University) for constructive and helpful review of the manuscript. We also appreciate critical discussions with J. Woo (Seoul National University), J. Hong (Kangwon National University), and J.-H. Lee (Chungnam National University) on the earlier version of the manuscript.

REFERENCES

An, T.X., Zhang, F., Xiang, W.D., Zhang, Y.Q., Xu, W.H., Zhang, H.J., Jiang, D.B., Yang, C.S., Lin, L.D., Cui, Z.T., and Yang, X.C., 1983, The Conodonts of North China and the Adjacent Regions. Science Press, Beijing, 223 p. (in Chinese)

Bauer, J.A., 2010, Conodonts and conodont biostratigraphy of the Joins and Oil Creek formations, Arbuckle Mountains, south-central Oklahoma. Bulletin of the Oklahoma Geological Survey, 150, 44 p.

Bergström, S.M., 2007, Middle and Upper Ordovician conodonts from the Fågelsång GSSP, Scania, southern Sweden. GFF, 129, 77–82.

Bergström, S.M. and Ferretti, A., 2017, Conodonts in Ordovician biostratigraphy. Lethaia, 50, 424–439.

Bergström, S.M., Finney, S.C., Chen, X., Pålsson, C., Wang, Z.H., and Grahn, Y., 2000, A proposed global boundary stratotype for the base of the Upper Series of the Ordovician System: The Fågelsång section, Scandia, southern Sweden. Episodes, 23, 102–109.

Bergström, S.M., Löfgren, A., and Maltez, J., 2004, The GSSP of the second (upper) stage of the Lower Ordovician Series: Diabasbrottet at Hunneberg, Province of Vaastergöland, southwest Sweden. Episodes, 27, 265–272.

Boggs Jr., S., 2014, Principles of Sedimentology and Stratigraphy (5th edition). Pearson Education, London, 565 p.

Choi, D.K., 1998, The Yongwol Group (Cambrian–Ordovician) redefined: a proposal for the stratigraphic nomenclature of the Choson Supergroup. Geosciences Journal, 2, 220–234.

Choi, D.K., Chough, S.K., Kwon, Y.K., Lee, S.-B., Woo, J., Kang, I., Lee, H.S., Lee, S.M., Sohn, Y.J., and Lee, D.-J., 2004, Taebaek Group (Cambrian–Ordovician) in the Seokgaejae section, Taebaeksan Basin: a refined lower Paleozoic stratigraphy in Korea. Geosciences Journal, 8, 125–151.

Chough, S.K., 2013, Geology and Sedimentology of the Korean Peninsula. Elsevier, London, 363 p.

https://doi.org/10.1007/s12303-020-0044-5

Cooper, J.D. and Keller, M., 2001, Palaeokarst in the Ordovician of the southern Great Basin, USA: implications for sea-level history. Sedimentology, 48, 855–873.

Cooper, R.A., Nowlan, G.S., and Williams, H.S., 2001, Global stratotype section and point for base of the Ordovician System. Episodes, 24, 19–28.

Cooper, R.A., Sadler, P.M., Hammer, O., and Gradstein, F.M., 2012, The Ordovician Period. In: Gradstein, F.M., Ogg, J.G., Schmitz, M.D., and Ogg, G.M. (eds.), The Geologic Time Scale, Elsevier, p. 489–523.

Desrochers, A. and James, N.P., 1988, Early Paleozoic surface and subsurface palaeokarst: Middle Ordovician carbonates, Mingan Islands, Quebec. In: James, N.P. and Choquette, P.W. (eds.), Paleokarst. Springer, New York, p. 183–210.

Dix, G.R., Robinson, G.W., and McGregor, D.C., 1998, Paleokarst in the Lower Ordovician Beekmantown Group, Ottawa Embayment: structural control inboard of the Appalachian orogen. Geological Society of America Bulletin, 110, 1046–1059.

Ethington, R.L. and Clark, D.L., 1981, Lower and Middle Ordovician conodonts from the Ibex area, western Millard County, Utah. Bringham Young University Geology Studies, 28, 160 p.

Goldman, D., Leslie, S.A., Nõlvak, J., Young, S., Bergström, S.M., and Huff, W.D., 2007, The global stratotype section and point (GSSP) for the base of the Katian Stage of the Upper Ordovician Series at Black Knob Ridge, southeastern Oklahoma, USA. Episodes, 30, 258–270.

Hwang, I.S., 1986, A study on stratigraphy and paleontology of the Maggol Formation of the Joseon Supergroup in Sangdong area, Yeongwolgun, Gangwondo, South Korea. MS. Thesis, Yonsei University, Seoul, 95 p. (in Korean with English abstract)

Jing, X., Zhou, H., and Wang, X., 2015, Ordovician (middle Darriwilian–earliest Sandbian) conodonts from the Wuhai area of Inner Mongolia, North China. Journal of Paleontology, 89, 768–790.

Kim, H.S., Choh, S.-J., Lee, J.-H., and Kim, S.J., 2019, Sediment grain size dose matter: implications of spatiotemporal variations in detrital zircon provenance for early Paleozoic peri-Gondwana reconstructions. International Journal of Earth Science, 108, 1–18.

Kim, J.Y., Kwon, J.Y., Kim, K.-S., and Cho, H.S., 2005, Graptolites from the Jigunsan Shale of Taebaeg Area, Korea. Journal of Korean Earth Science Society, 26, 137–148.

Kim, K.H., Choi, D.K., and Lee, C.Z., 1991, Trilobite biostratigraphy of the Dumugol Formation (Lower Ordovician) of Dongjeom Area, Korea. Journal of the Paleontological Society of Korea, 7, 106–115.

Kim, S.H., 1987, A study on stratigraphy and paleontology of Maggol limestone distributed in the south part of the Baegunsan Syncline. MS. Thesis, Yonsei University, Seoul, 131 p. (in Korean with English abstract)

Knight, I., James, N.P., and Lane, T.E., 1991, The Ordovician St. George Unconformity, northern Appalachians: The relationship of plate convergence at the St. Lawrence Promontory to the Sauk/Tippecanoe sequence boundary. Geological Society of America Bulletin, 103, 1200–1225.

Kwon, K.-R., 2007, Early Ordovician Graptolites from the Dumugol Shale of Taebaek Area, Korea. MS. Thesis, Korea National University of Education, Cheongju, 113 p.

Kwon, Y.K., Lee, D.-J., Choi, D.K., and Chough, S.K., 2003, Lower Ordovician sponge bioherms in the Makkol Formation, Taebaeksan Basin, Mideast Korea. Facies, 48, 79–90.

Lee, B.-S., 1992, Additional conodonts from the Cambrian–Ordovician boundary beds in the Baegunsan syncline. Journal of the Geological Society of Korea, 28, 590–603.

Lee, B.-S., 2014, Conodonts from the Sesong Slate and Hwajeol Formation (Guzhangian to Furongian) in the Taebaeksan Basin, Korea. Acta Geologica Sinica, 88, 35–45.

Lee, B.-S., 2019, Upper Ordovician (Sandbian) conodonts from the Hoedongri Formation of western Jeongseon, Korea. Geosciences Journal, 23, 695–705.

Lee, B.-S. and Bak, Y.-S., 2015, Revision of the conodont zonation of the uppermost Hwajeol Formation (Furongian), Taebaeksan Basin, Korea. Geosciences Journal, 19, 621–630.

Lee, B.-S. and Lee, J.-D., 1999, Conodonts from the Mungog Formation (Lower Ordovician), Yeongweol. Journal of Paleontological Society of Korea, 15, 21–42.

Lee, B.-S. and Seo, K.-S., 2004, Lower Paleozoic conodonts of Korea. Paleontological Society of Korea, Special Publication, 7, 189–215.

Lee, D.-C. and Choi, D.K., 1992, Reappraisal of the Middle Ordovician trilobites from the Jigunsan Formation, Korea. Journal of the Geological Society of Korea, 28, 167–183.

Lee, D.-C., Choh, S.-J., Lee, D.-J., Ree, J.-H., Lee, J.-H., and Lee, S.-B., 2017, Where art thou "great hiatus? – review of Late Ordovician to Devonian fossil-bearing strata in the Korean Peninsula and its tectonostratigraphic implications. Geosciences Journal, 21, 913–931.

Lee, H.Y., Lee, K.J., and Yi, M.S., 1993, Conodonts from the lower Paleozoic strata in Mungyeong area, Gyeongsangbuk-do, Korea, and their biostratigraphic and bioprovincial implications. Journal of the Geological Society of Korea, 29, 507–523.

Lee, K.W., 1986, A study on stratigraphy and paleontology of the upper Joseon Supergroup in Jangseong-Dongjeom area, Taebaeg city, Gangwon-do. MS. Thesis, Yonsei University, Seoul, 101 p. (in Korean with English abstract)

Lee, K.W. and Lee, H.-Y., 1990, Conodont biostratigraphy of the upper Choseon Supergroup in Jangseong-Dongjeom area, Gangweon-do. Journal of the Paleontological Society of Korea, 6, 188–210.

Lee, S.J., 1990, Conodont biostratigraphy and paleontology of the Lower Paleozoic Youngheung Formation in the Yeongweol Area, Kangweondo, Korea. MS. Thesis, Yonsei University, Seoul, 107 p. (in Korean with English abstract)

Lee, Y.N. and Lee, H.-Y., 1986, Conodont biostratigraphy of the Jigunsan shale and Duwibong limestone in the Nokjeon-Sangdong area, Yeongweol-gun, Kangweondo, Korea. Journal of the Paleontological Society of Korea, 2, 114–136.

Lee, Y.T., 2009, A study on classification and biostratigraphy on conodonts from the Maggol Formation in the Seokgaejae area, Kangwondo, Korea. MS. Thesis, Kongju National University, Kongju, 60 p. (in Korean with English abstract)

Miller, J.F., Evans, K.R., Loch, J.D., Ethington, R.L., Stitt, J.H., Holmer, L., and Popov, L.E., 2003, Stratigraphy of the Sauk III interval (Cambrian–Ordovician) in the Ibex Area, western Millard Country, Utah and central Texas. Brigham Young University Geology Studies, 47, 23–118.

Mussman, W.J. and Read, J.F., 1986, Sedimentology and development of a passive- to convergent-margin unconformity: Middle Ordovician Knox unconformity, Virginia Appalachians. Geological Society of America Bulletin, 97, 282–295.

Paik, I.S., 1987, Depositional environments of the Middle Ordovician Maggol Formation, southern part of the Baegunsan syncline area. Journal of the Geological Society of Korea, 23, 360–373.

Repetski, J.E. and Ethington, R.L., 1983, *Rossodus manitouensis* (Conodonta), a new Early Ordovician index fossil. Journal of Paleontology, 57, 289–301.

Saltzman, M.R., Edwards, C.T., Leslie, S.A., Dwyer, G.S., Bauer, J.A., Repetski, J.E., Harris, A.G., and Bergström, S.M., 2014, Calibration of a conodont apatite-based Ordovician $^{87}Sr/^{86}Sr$ curve to biostratigraphy and geochronology: implications for stratigraphic resolution. Geological Society of America Bulletin, 126, 1551–1568.

Seo, K.-S. and Lee, B.-S., 2010, Conodonts from the Early Ordovician Dumugol Formation in Seokgaejae area, Bonghwagun, Kyungsangbukdo, Korea. Journal of the Paleontological Society of Korea, 26, 59–69. (in Korean with English abstract)

Seo, K.-S., Lee, H.-Y., and Ethington, R.L., 1994, Early Ordovician conodonts from the Dumugol Formation in the Baegunsan Syncline, eastern Yeongweol and Samcheog areas, Kangweon-do, Korea. Journal of Paleontology, 68, 599–616.

Stouge, S., 1984, Conodonts of the Middle Ordovician Table Head Formation, Western Newfoundland. Fossils and Strata, 16, 160 p.

Wang, C.Y. and Wang, Z.H., 1983, Review of conodont biostratigraphy in China. Fossils and Strata, 15, 29–33.

Wang, Z.H., Bergström, S.M., and Lane, R.H., 1996, Conodont provinces and biostratigraphy in Ordovician of China. Acta Palaeontologica Sinica, 35, 26–59.

Wang, Z.H., Bergström, S.M., Zhen, Y.Y., Chen, X., and Zhang, Y.D., 2013, On the integration of Ordovician conodont and graptolite biostratigraphy: new examples from Gansu and Inner Mongolia in China. Alcheringa, 37, 510–528.

Wang, Z.H., Bergström, S.M., Zhen, Y.Y., Zhang, Y., and Wu, R.C., 2014, A revision of the Darriwilian biostratigraphic conodont zonation in Tangshan, Hebei Province based on new conodont collections. Acta Palaeontologica Sinica, 53, 1–15. (in Chinese with English abstract)

Wang, Z.H., Zhen, Y.Y., Bergström, S.M., Wu, R.C., Zhang, Y.D., and Ma, X., 2019, A new conodont biozone classification of the Ordovician System in South China. Palaeoworld, 28, 173–186.

Wang, Z.H., Zhen, Y.Y., Bergström, S.M., Zhang, Y.D., and Wu, R.C., 2018, Ordovician conodont biozonation and biostratigraphy of North China. Australasian Palaeontological Memoirs, 51, 65–79.

Wang, Z.H., Zhen, Y.Y., Zhang, Y.D., and Wu, R.C., 2016, Review of the Ordovician conodont biostratigraphy in the different facies of North China. Journal of Stratigraphy, 40, 1–16. (in Chinese with English abstract)

Woo, K.S., 1999, Cyclic tidal successions of the Middle Ordovician Maggol Formation in the Taebaeg area, Kangwondo, Korea. Geosciences Journal, 123–140.

Yun, C.-S., 1999, Ordovician cephalopods from the Maggol Formation of Korea. Paleontological Research, 3, 202–221.

Zhang, S.X. and Zhen, Y.Y., 1991, China. In: Moullade, M. and Nairn, A.E.M. (eds.), The Phanerozoic Geology of the World I, the Palaeozoic A. Elsevier Science Publishers, Amsterdam, p. 219–274.

Zhen, Y.Y. and Percival, I.G., 2017, Late Ordovician conodont biozonation of Australia – current status and regional biostratigraphic correlations. Alcheringa, 41, 285–305.

Zhen, Y.Y., Percival, I.G., and Zhang, Y.D., 2015, Floian (Early Ordovician) conodont-based biogeography and biostratigraphy of the Australasian Superprovince. Palaeoworld, 24, 100–109.

Zhen, Y.Y., Zhang, Y.D., Tang, Z.C., Percival, I.G., and Yu, G.H., 2014, Early Ordovician conodonts form Zhejiang Province, southeast China and their biostratigraphic and palaeobiogeographic implications. Alcheringa, 39, 109–141.

Zhen, Y.Y., Zhang, Y., Wang, Z., and Percival, I.G., 2016, Huaiyuan Epeirogeny – shaping Ordovician stratigraphy and sedimentation on the North China Platform. Palaeogeography, Palaeoclimatology, Palaeoecology, 448, 363–370.

Zheng, Y.F., Xiao, W.J., and Zhao, G.C., 2013, Introduction to tectonics of China. Gondwana Research, 23, 1189–1206.

https://doi.org/10.1007/s12303-020-0044-5